SUPPLEMENTARY INFORMATION for

Combined emergent constraints on future extreme precipitation changes

Hideo Shiogama[1*], Michiya Hayashi[1], Nagio Hirota[1], Tomoo Ogura[1], Hyungjun Kim[2, 3, 4, 5] & Masahiro Watanabe[6]

[1]Earth System Division, National Institute for Environmental Studies, Tsukuba, Japan

[2]Moon Soul Graduate School of Future Strategy, Korea Advanced Institute of Science and Technology, Daejeon, Korea

[3]Graduate School of Data Science, Korea Advanced Institute of Science and Technology, Daejeon, Korea

[4]Department of Civil and Environmental Engineering, Korea Advanced Institute of Science and Technology, Daejeon, Korea

[5]Graduate School of Green Growth and Sustainability, Korea Advanced Institute of Science and Technology, Daejeon, Korea

[6]Atmosphere and Ocean Research Institute, University of Tokyo, Kashiwa, Japan

[*]Corresponding author: Hideo Shiogama, shiogama.hideo@nies.go.jp

Content:

Supplementary Table 1 | Analyzed earth system models and their ensemble sizes.

CMIP5 model name	Ens. size for RCP4.5 (RCP8.5)			CMIP6 model name	Ens. size for SSP2-4.5 (SSP5-8.5)		
	R	*T*	*Q*		*R*	*T*	*Q*
ACCESS1-0	1 (1)	1 (1)	1 (0)	ACCESS-CM2	5 (1)	5 (1)	5 (0)
ACCESS1-3	1 (1)	1 (1)	1 (0)	ACCESS-ESM1-5*	36 (1)	36 (1)	30 (0)
CCSM4	2 (2)	2 (2)	0 (0)	BCC-CSM2-MR	1 (1)	1 (1)	1 (0)
CESM1-BGC	1 (1)	1 (1)	0 (0)	CMCC-CM2-SR5	1 (1)	1 (1)	1 (0)
CESM1-CAM5	1 (1)	1 (1)	1 (0)	CMCC-ESM2	1 (1)	1 (1)	1 (0)
CMCC-CM	1 (1)	1 (1)	0 (0)	CNRM-CM6-1	1 (1)	1 (1)	1 (0)
CMCC-CMS	1 (1)	1 (1)	0 (0)	CNRM-ESM2-1	1 (1)	1 (1)	1 (0)
CNRM-CM5	1 (1)	1 (1)	1 (0)	CanESM5*	25(25)	25(25)	24(0)
CSIRO-Mk3-6-0	10(10)	10(10)	10(0)	EC-Earth3	18 (1)	18 (1)	17 (0)
CSIRO-Mk3L-1-2	3 (0)	3 (0)	0 (0)	EC-Earth3-CC	1 (1)	1 (1)	1 (0)
CanESM2	5 (5)	5 (5)	5 (0)	EC-Earth3-Veg	6 (1)	6 (1)	6 (0)
EC-EARTH	4 (5)	4 (5)	0 (0)	EC-Earth3-Veg-LR	3 (1)	3 (1)	3 (0)
GISS-E2-R	1 (0)	1 (0)	1 (0)	GFDL-CM4	1 (1)	1 (1)	1 (0)
IPSL-CM5A-LR	4 (4)	4 (4)	4 (0)	GFDL-ESM4	1 (1)	1 (1)	1 (0)
IPSL-CM5A-MR	1 (1)	1 (1)	1 (0)	HadGEM3-GC31-LL	4 (1)	4 (1)	3 (0)
IPSL-CM5B-LR	1 (1)	1 (1)	1 (0)	INM-CM4-8	1 (1)	1 (1)	1 (0)
MIROC-ESM	1 (1)	1 (1)	1 (0)	INM-CM5-0	1 (1)	1 (1)	1 (0)
MIROC-ESM-CHEM	1 (1)	1 (1)	1 (0)	IPSL-CM6A-LR	8 (1)	8 (1)	0 (0)
MIROC5	3 (3)	3 (3)	3 (0)	KACE-1-0-G	3 (1)	3 (1)	1 (0)
MPI-ESM-LR	3 (3)	3 (3)	0 (0)	KIOST-ESM	1 (1)	1 (1)	1 (0)
MPI-ESM-MR	3 (1)	3 (1)	0 (0)	MIROC-ES2L*	30 (1)	30 (1)	30 (0)
MRI-CGCM3	1 (1)	1 (1)	1 (0)	MIROC6*	50(50)	50(50)	7 (0)
NorESM1-M	1 (1)	1 (1)	1 (0)	MPI-ESM1-2-HR	2 (1)	2 (1)	2 (0)
bcc-csm1-1	1 (1)	1 (1)	1 (0)	MPI-ESM1-2-LR*	30 (1)	30 (1)	30 (0)
bcc-csm1-1-m	1 (1)	1 (1)	1 (0)	MRI-ESM2-0	1 (1)	1 (1)	1 (0)
inmcm4	1 (1)	1 (1)	1 (0)	NESM3	1 (1)	1 (1)	0 (0)
				NorESM2-LM	3 (1)	3 (1)	3 (0)
				NorESM2-MM	2 (1)	2 (1)	2 (0)
				TaiESM1	1 (1)	1 (1)	1 (0)
				UKESM1-0-LL	9 (1)	9 (1)	3 (0)

Asterisks indicate that 25 members of each of these models (historical + SSP2-4.5) are used for estimating the standard deviation of the internal variability.

Supplementary Table 2 | Raw and constrained ranges of the global mean extreme precipitation change (ΔR_{gm}, mm/day) and the relative reduction of variance (RRV, %) (CMIP5&6, RCP8.5/SSP5-8.5)

	50th percentile (mm/day)	2.5th percentile (mm/day)	97.5th percentile (mm/day)	RRV (%)
Raw	8.87	0.557	17.2	-
ΔT_{gm}-related EC	8.03	0.708	15.4	22
$\frac{\Delta R_{gm}}{\Delta T_{gm}}$-related EC	8.30	2.10	16.7	20
Combined EC	7.99	2.13	15.4	37

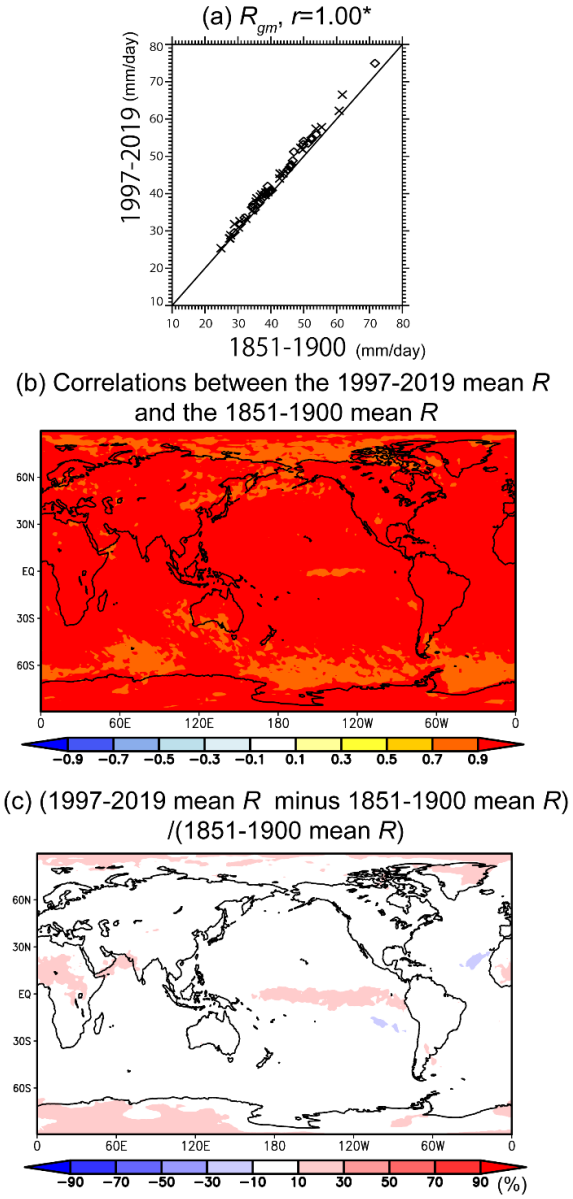

Supplementary Figure 1 | Sensitivities of the climatological values of global mean and regional extreme precipitation (R_{gm} and R). (a) Horizontal axes indicate the 1851-1900 average values of R_{gm} (mm/day). Vertical axes show the corresponding 1997-2019 mean values (mm/day). Crosses and diamonds are the CMIP5 and CMIP6 earth system models (ensemble mean of each model), respectively. Pearson's correlation is denoted at the top of the panel. Asterisks indicate that this correlation is significant at the 5% level. (b) Pearson's correlations between the 1997-2019 mean regional R and the 1851-1900 mean R. (c) Percentage differences of the multi-model-averaged 1997-2019 mean R and the 1851-1900 mean R (% of the 1851-1900 mean values).

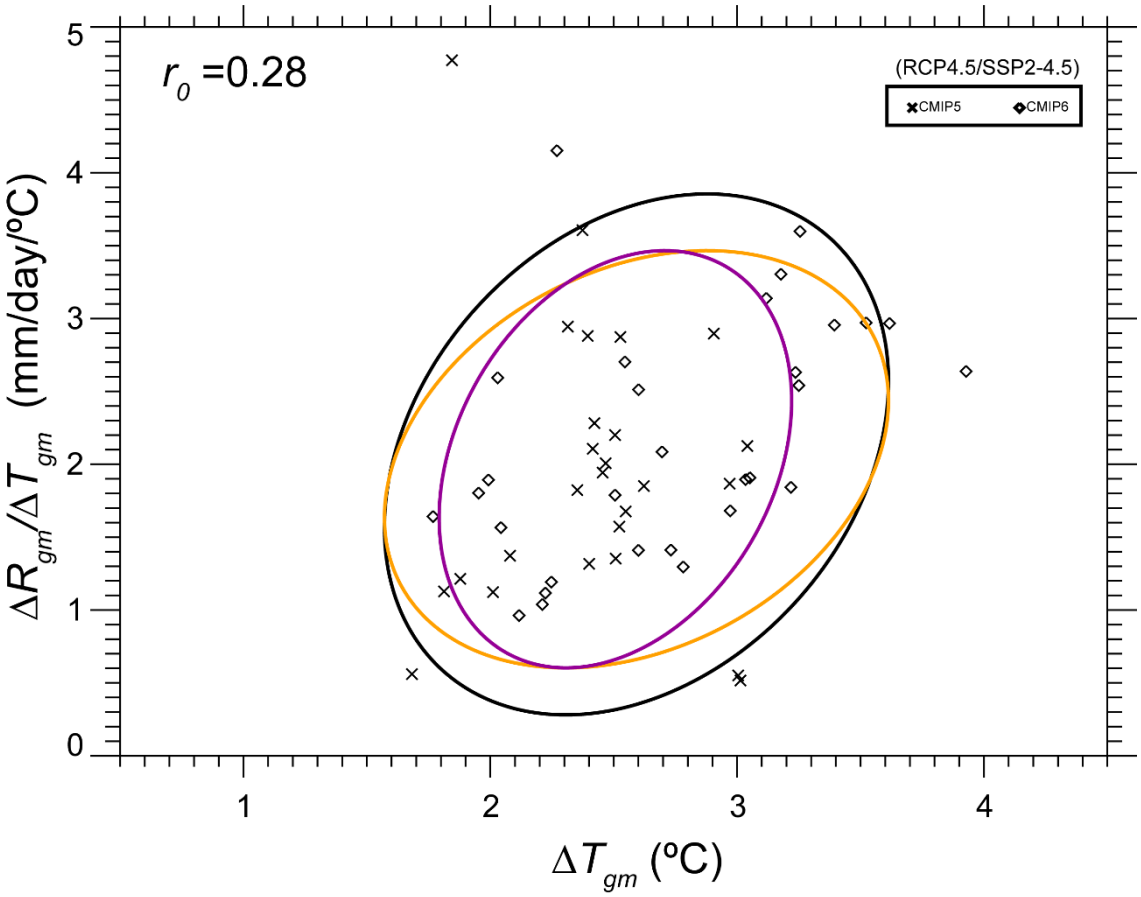

Supplementary Figure 2 | Ellipses of the joint normal distributions of the global mean temperature change (ΔT_{gm}) and the extreme precipitation sensitivity ($\frac{\Delta R_{gm}}{\Delta T_{gm}}$).

Horizontal and vertical axes indicate ΔT_{gm} (°C) and $\frac{\Delta R_{gm}}{\Delta T_{gm}}$ (mm/day/°C), respectively. Crosses and diamonds denote the CMIP5 and CMIP6 earth system models (ensemble mean of each model), respectively. Pearson's correlation (r_0) is provided in the panel. Two standard deviation ellipses are shown for (black) the combination of the raw ΔT_{gm} and the raw $\frac{\Delta R_{gm}}{\Delta T_{gm}}$, (orange) the combination of the raw ΔT_{gm} and the constrained $\frac{\Delta R_{gm}}{\Delta T_{gm}}$ and (purple) the combination of the constrained ΔT_{gm} and the constrained $\frac{\Delta R_{gm}}{\Delta T_{gm}}$, respectively.

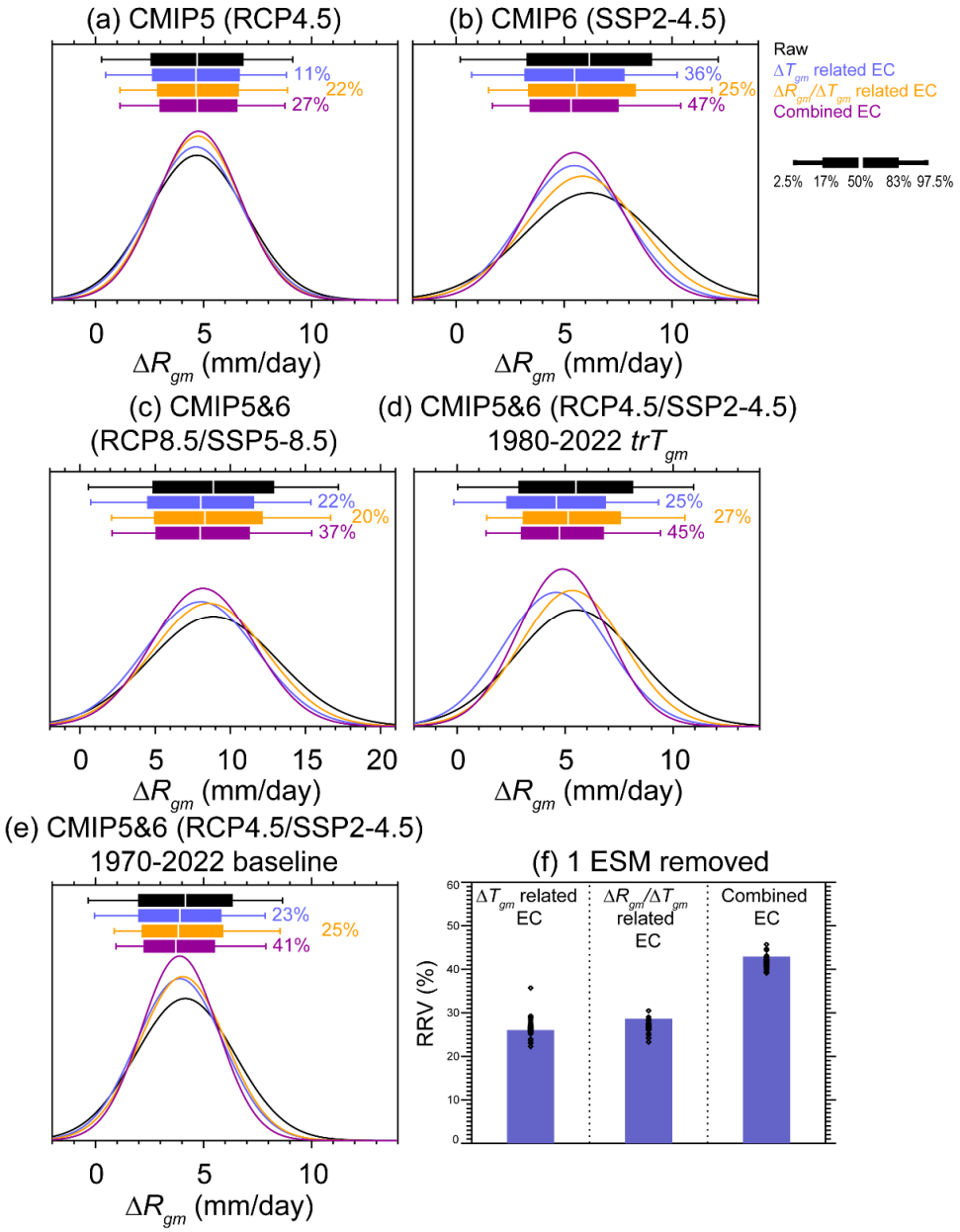

Supplementary Figure 3 | Sensitivity tests of emergent constraints on the global mean extreme precipitation change (ΔR_{gm}). Same as Fig. 2 but for (**a**) CMIP5-only (RCP4.5), (**b**) CMIP6-only (SSP2-4.5), and (**c**) CMIP5 (RCP8.5) and CMIP6 (SSP5-8.5). **d** Same as Fig. 2 but using the 1980-2022 global mean temperature trend (trT_{gm}) instead of the 1970-2022 value. **e** Same as Fig. 2 but using the 1970-2022 baseline instead of the 1851-1900 value. **f** Blue bars indicate the relative reduction of variance (RRV) when we use all the earth system models (ESMs) (the same numbers shown in Fig. 2). Diamonds show the RRVs for the sensitivity tests of redoing the EC calculations with each of the ESMs omitted.

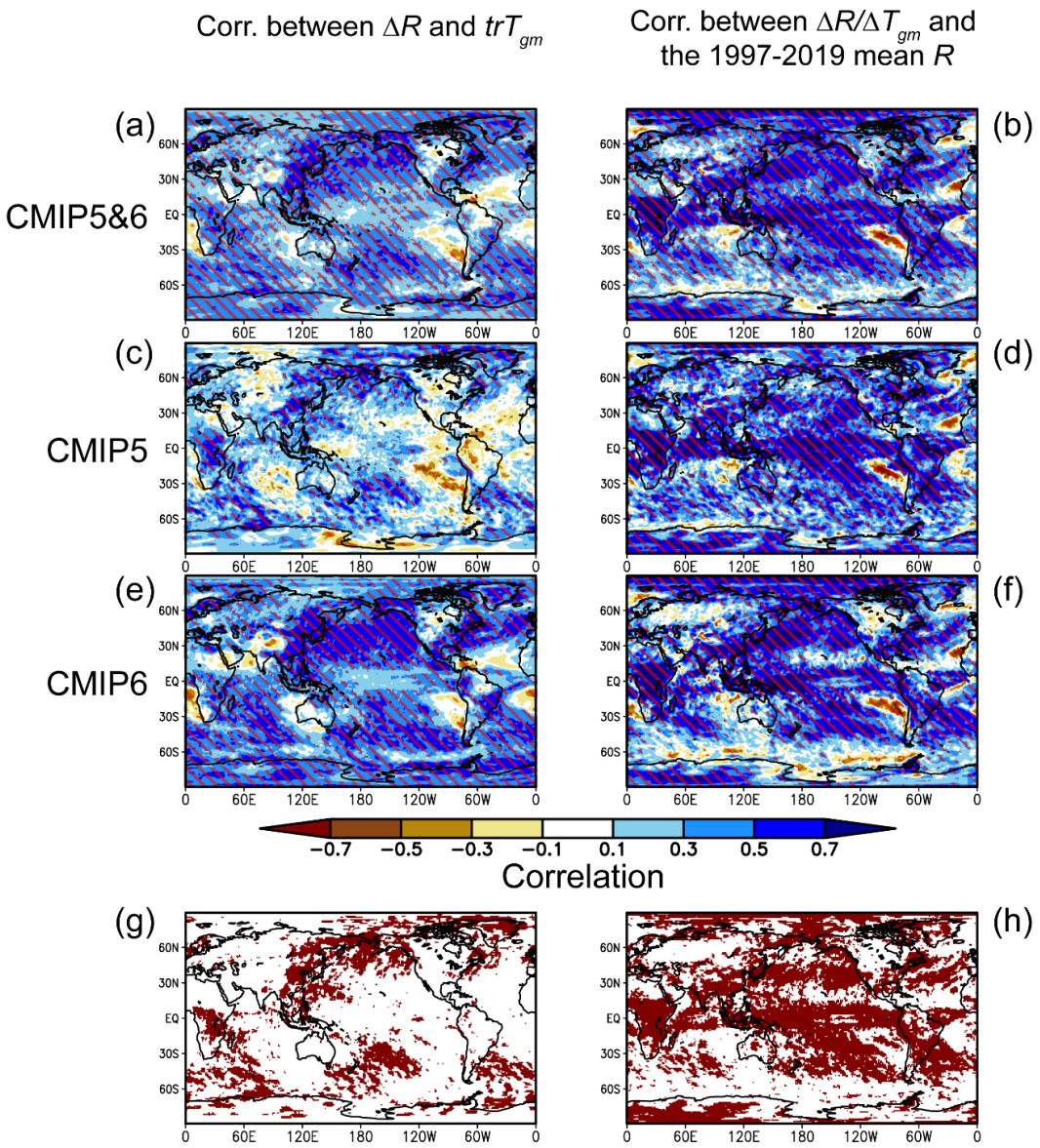

Supplementary Figure 4 | Correlations between future changes and past climate. Pearson's correlations (**a**) between the regional extreme precipitation change (ΔR) and the past temperature trend (trT_{gm}) and (**b**) between the extreme precipitation sensitivity ($\frac{\Delta R}{\Delta T_{gm}}$) and the 1997-2019 mean R for the CMIP5 and CMIP6. Red hatches indicate significant correlations at the ±5% levels. **c-d** The same as the panels (**a-b**), but for the CMIP5-only. **e-f** The same as the panels (**a-b**), but for the CMIP6-only. The bottom panels show the grids where the correlations (**g**) between ΔR and trT_{gm} and (**h**) between $\frac{\Delta R}{\Delta T_{gm}}$ and the 1997-2019 mean R are significant for both the CMIP5-only and CMIP6-only.

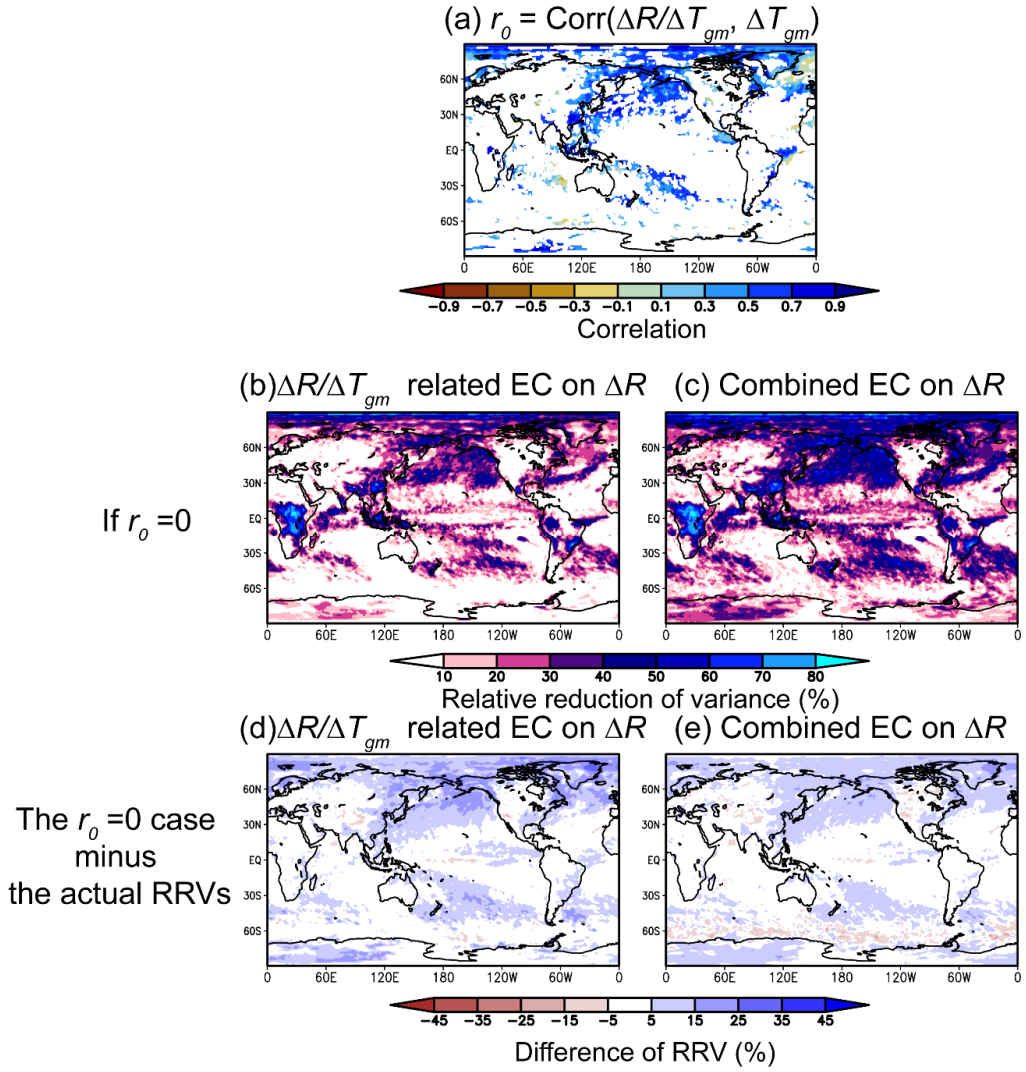

Supplementary Figure 5 | Tests of ignoring correlations between the regional extreme precipitation sensitivity ($\frac{\Delta R}{\Delta T_{gm}}$) and the global mean temperature change (ΔT_{gm}) on the regional relative reduction of variance (RRV). a Correlations between $\frac{\Delta R}{\Delta T_{gm}}$ and ΔT_{gm} (r_0). Only significant correlations at the ±5% levels are drawn. Panels (**b-c**) show RRVs (%) for (**b**) the $\frac{\Delta R}{\Delta T_{gm}}$-related EC and (**c**) the combined EC in the case that r_0 is set to zero. Panels (**d-e**) denote the difference of RRVs (%) between the case that r_0 is set to zero and the actual RRVs for (**d**) the $\frac{\Delta R}{\Delta T_{gm}}$-related EC and (**e**) the combined EC.

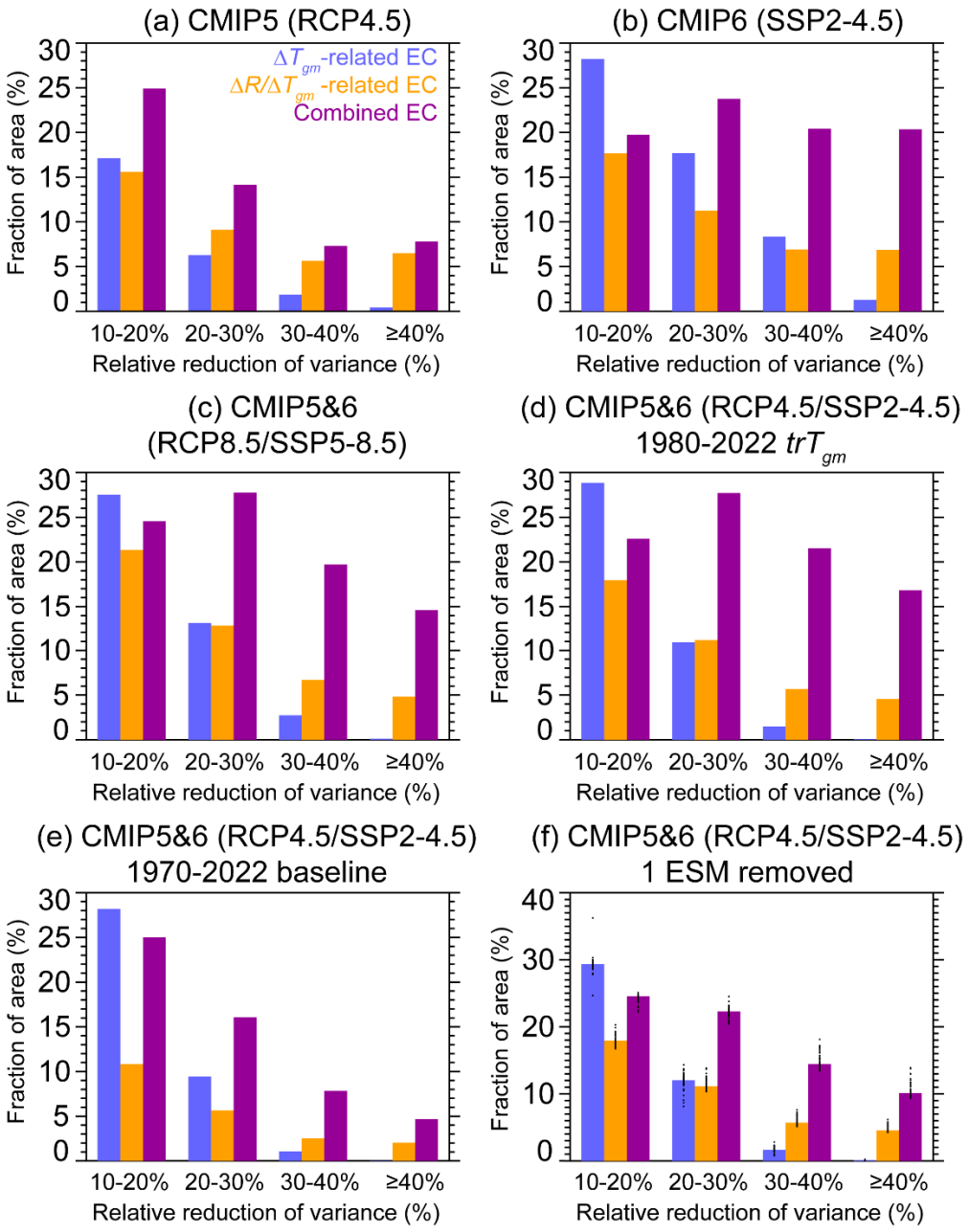

Supplementary Figure 6 | Sensitivity tests of the fraction of the global area with given relative reduction of variance (RRV) values. Same as Fig. 4f but for (**a**) CMIP5-only (RCP4.5), (**b**) CMIP6-only (SSP2-4.5), and (**c**) CMIP5 (RCP8.5) and CMIP6 (SSP5-8.5). **d** Same as Fig. 4f but using the 1980-2022 global mean temperature trend (trT_{gm}) instead of the 1970-2022 value. **e** Same as Fig. 4f but using the 1970-2022 baseline instead of the 1851-1900 value. **f** Dots show the fractions for the sensitivity tests of redoing the EC calculations with each of the earth system models (ESMs) omitted. Bars indicate the fractions when we use all the ESMs (the same as Fig. 4f). Note that the range of the vertical axis of the panel (**f**) is different from that of the other panels and Fig. 4f.

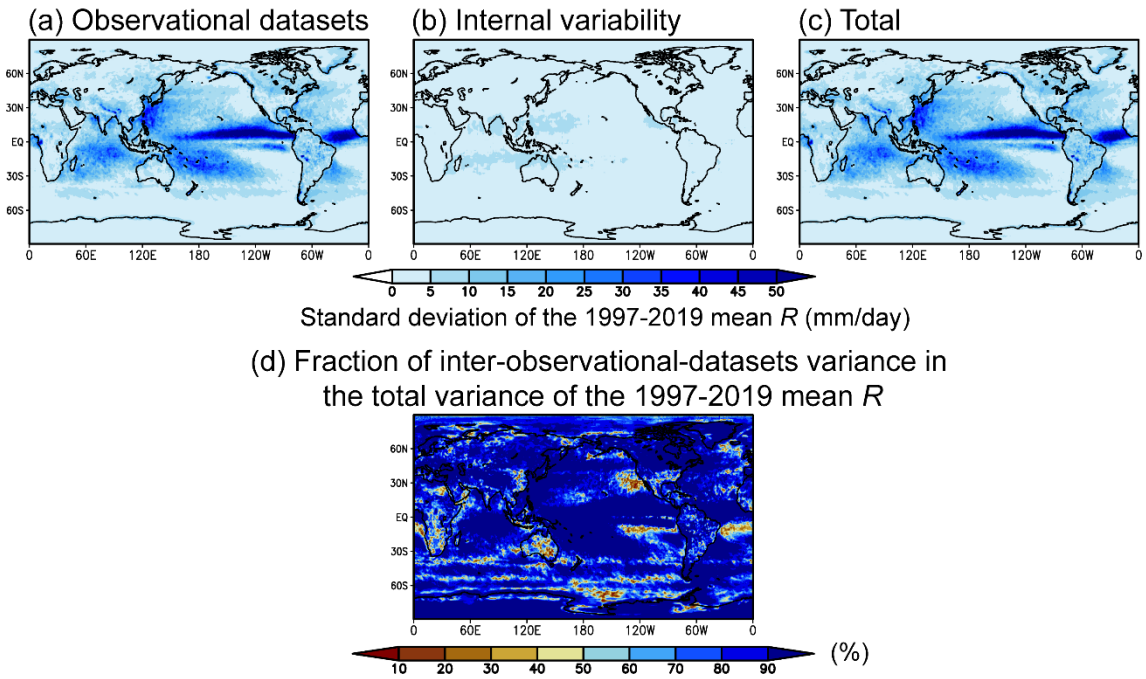

Supplementary Figure 7 | Uncertainties of the 1997-2019 mean extreme precipitation (*R*). Panels (**a-c**) show the standard deviation of the 1979-2019 mean *R* (mm/day) from (**a**) differences between the observational datasets, (**b**) internal climate variability and (**c**) both factors (inter-observation-datasets + internal climate variability), respectively. **d** Fractions of the inter-observation-datasets variance in the total variance (%).